Low Frequency Bottom Reflectivity from Reflection

*,Alexander Kritski[1]*and Chris Jenkins[2]*

[1]*School of Geosciences, University of Sydney, NSW,* [2]*Ocean Sciences Institute, University of Sydney, NSW.*

Abstract

Ocean bottom reflectivity has been studied for a simple layered sedimentary model at shallow depth. Reflections from the bottom were determined from standard geophysical reflection data. The plane wave reflections have been obtained as bottom loss (-20log|R|) from the available reflection seismic data. Bottom loss estimated in the 10-250 Hz band are presented as functions of frequency and of angle of incidence (relative to horizontal) and are shown to depend on the properties of the layered ocean bottom. In the bottom loss results, a critical angle is observed which decreases from about 39° at 40-10 Hz to about 20° at 240 Hz. This critical angle is most likely associated with the reflection of compressional waves near the ocean-sediment interface. The frequency dependence indicates that the lower frequencies interact with a deeper sediment layer of greater sound speed than the near-surface sediments. At about 59° there is an indication of another critical angle, possibly due to reflection from the substrate beneath the sediments. The significance of these results is that reflection seismic data can be used to derive inputs for naval sonar prediction models, especially in the frequency range of passive sonars.

Indroduction

Plane-wave reflection and refraction coefficients play an important role in the interpretation of acoustic data in modern marine seismology. These coefficients are generally based on the partitioning of energy at the interface between water and an elastic solid , and the result is the classical Rayleigh reflection and transmission coefficients that relate to the amplitudes of homogeneous incident waves and homogeneous reflected and refracted waves. For the case of an elastic solid, only two kinds of body wave can propagate and the particle motion is either parallel or perpendicular to the wave normal depending on whether a dilatational or shear wave is being considered. The angles of incidence and emergence are related by Snell's law and when one of the angles corresponding to a reflected or refracted wave increases to 90°, a "critical" angle of incidence is defined for the generating wave.

When the angle of incidence of the generating wave exceeds a critical angle, the body wave which has become parallel to the interface no longer propagates and an interface wave is necessary to satisfy the boundary conditions. This wave decays exponentially away from the interface and its phase velocity is determined by the phase velocity of the generating wave projected onto the interface.

A more realistic model of the sediments would include a viscous-elastic or porous viscous-elastic material rather then the elastic one. In this case there are fundamental differences in the response at the interface between water and sediment or/and between two different kinds of sediments. Reflected and refracted waves are rather inhomogeneous in the sense that the wave amplitudes vary in planes of constant phase and the trajectory of particle motion is elliptic in shape rather than parallel or perpendicular to the direction of the wave normal [8].

The reflectivity data used in the present work have been collected in experiments where receivers were located near the sea surface [1]. The geophysical information related to the all kinds of inhomogeneous waves including interface waves is not available at the receiving point as only compressional waves can propagate in the water column to reach the receivers.

In this work the simple layered model has been suggested. The ocean is described by a constant sound speed half space, the bottom is described by a near surface sediment layer (200-300m depth) of constant sound speed gradient overlying another solid half space (low sediments, and then crust) of constant sound speed.

The results of the reflectivity estimation, however, indicate that reflection coefficients become frequency dependent in a quite complex way. This effect might indicate viscous losses in the sediment layer or/and multilayering. Thus the bottom reflectivity measured from the interface for a simple model (homogeneous sediment layer with constant speed and attenuation) indicates that the properties of near-surface sediments fit a viscous-elastic model.

Seismic reflection experiment

Experimental setup

The reflection seismic data used in these studies was collected from North West shelf area in the North Bonaparte Basin which situates between NW margin and the Timor Trough (Australian Geological Survey

*Currently with Centre for Marine Science & Technology, Curtin University of Technology

Organisation, Timor Tie survey 118/8). The approximate depth in this area is about 150m. The range of frequencies: 10 Hz up to 240 Hz. The high frequencies are limited due to the experiment conditions. A total of 272.1 km of data were acquired along transect. The data contains 584 shot points and 116800 traces. Detailed information on the geometry and method of the experiment is presented in *Kritski & Jenkins* [7].

The bottom reflectivity data used in this work have been collected during the standard seismic reflection survey carried out with one ship (Figure 1).
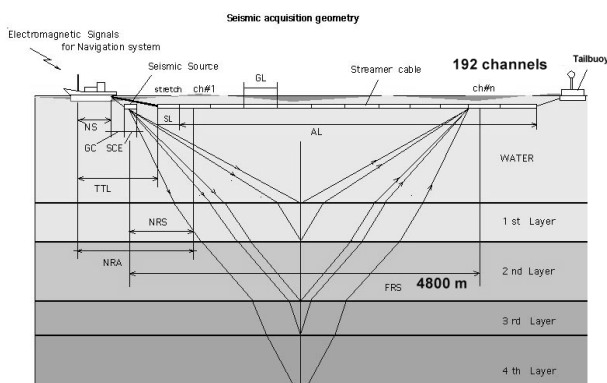
Figure 1. Seismic acquisition geometry.

The ship was towing an array of hydrophones which was suspended from a free floating tailbuoy at a depth of about 12 m. The total active section length of the array was 4800m with 192 active channels (Shot interval - 50m). Taking into account the geometry of the data collecting experiment covers the region of grazing (i.e., incidence) angles from 10^0-77^0. Calculations were carried out assuming that the bottom was a horizontally stratified medium.

Source data

The seismic reflection data we analysed in this work was obtained using a sleeve gun array (capacity 50 litres, 3000 cu in) [1]. Further details of which are given in *Kritski & Jenkins* [7]. Analysis of the far field signature of the gun and its spectrum are presented in *Kritski & Jenkins* [7]. The duration of the pressure pulse is about 96 ms. The source spectrum has useful components between 35 and 250 Hz.

Aside from using the far-field source signature in the calculations, no allowance was made for effects of seasurface reflection on the water-borne signal. A more detailed treatment would have required special inputs on sea state and deducted acoustic prediction modelling. Signal-to-noise ratio for the data was estimated from non-shot interval of each record. The average S/N ratio was 20–25 dB.

Geophysical data

Geopgysical data used in our studies are typical Common Shot Point (CSP) data. They are of variable quality, being subject to several types of noise of different origins [4,6]. Reflectors are recognised in these plots by their hyperbolic traveltimes. If the reflecting surface is horizontal then the apex of the reflection hyperbola is situated at zero offset. On the other hand if it is a dipping interface, then the reflection hyperbola is skewed in the undip direction (Details in [7]).

Figure 2 shows a variety of wave types at shallow depth (up to 2 sec two-way travel time) which corresponds to arrivals from the sedimentary structure.
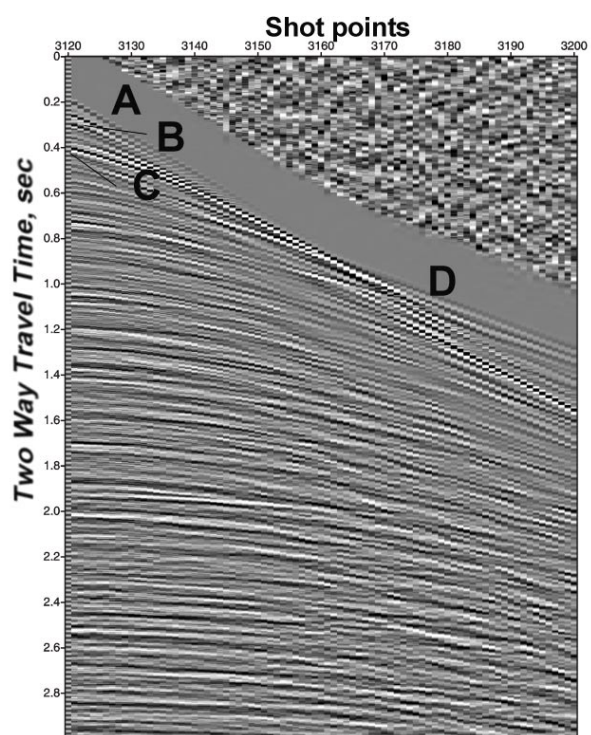

Figure 2 Example of Shot Point data

Direct arrivals *A* are significantly suppressed by receiver arrays in the field. *B* represents water bottom reflection on short-offset traces. Note the shallow reflector *C* and associated refraction arrival *D*. At about 0.7sec another reflector is seen. Much of the energy between 0.8 and 2 sec is most likely multiples associated with *B*, *C* and *E* arrivals. Linear noise (possibly cable noise) and low frequency noise (possibly propeller noise) appear in the deeper portions of the records.

Methods and programs for the reflection data reading and observations on the nature (sufficiency, quality) are presented in *Kritski, A. & Jenkins* [7].

Sesmic acoustic data

The data from three seismic shots were used for initial calculations. A 100000 traces were extracted form each individual shot, which allows to cover the region of grazing (i.e., incidence) angles from 10^0-77^0.

Signals recording amplitudes are normalized for source energy and spreading losses. For homogeneous medium without attenuation wave amplitudes decay as *(1/r)* where is the distance; energy decays as *1/(r^2)*. For a layered medium, amplitude decay can be described approximately by *1/[v^2*t]*, where *t* – two way travel time, *v* – average velocity of reflection. Thus, the gain function for geometric spreading is:

*g(t)=[v*v(t0)]^2[t/t(0)]*,

where *v(0)* is the velocity value at specified time *t(0)*.
The bottom reflected signal was obtained by windowing the seismic traces from each shot so as to select the first arrival that interacted only with the ocean bottom. Time window (70ms for long offset)s gives ~70m for the depth of interaction. The multiple filter technique was applied also to analyze seismic traces in terms of frequencies and arrival times [3] - as illustrated in Figure 4.
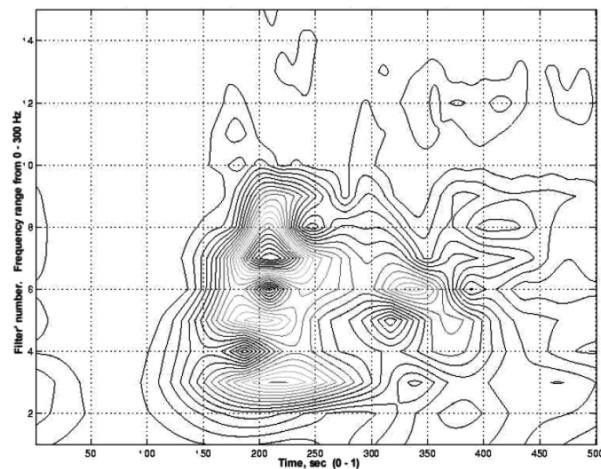

Figure 3. Example of multiple filter technique. Signals as a function of both time and frequency. The Y axis is in terms of Gaussian Frequency Window Number

The calculation uses a sequence of overlapping frequency windows, each window being a short frequency range compared to the whole spectrum range [3]. An amplitude spectrum was calculated from the windowed signals, using each window in turn. A Gaussian window function was used. The results are presented on a rectangular grid as a function of the time and of frequency (center of the each frequency window); the spectrum from each window contributes a column to the grid. The sonograms are obtained by contouring the resulting grid. The energy resulting from the sea floor reflection extends uniformly across the sonogram, at zero time, showing that the sea floor

is almost equally reflective across the frequency range. The bottom reflections can be readily identified in the sonogram. The pattern of the sonogram after the first arrivals is complex. Each trace record is shifted in time so that the first arrivals in the sonograms are shifted as well. Each trace record has been filtered then using a frequency window calculated from the multiple window analysis for the first bottom arrivals.

Bottom loss calculations

The bottom loss

The organization of seismic reflection records allows separation of the water arrivals and reflections from the bottom at close offsets. At large offsets water arrivals were estimated assuming linear propagation through water column (initial water signals have been estimated from close offsets were water arrivals can be geometrically picked up from the reflection record section).

The bottom reflected signal was found by using time windowing of the first bottom arrival to select the first arrival which interacted only with the ocean bottom. The length of the window varied from 130ms at the closest ranges to about 70ms at large offsets.

The bottom reflection loss was determined from the measured propagation loss of the bottom bounce paths by subtracting an estimate of the water column loss along the paths. In this approach, the estimates of water column propagation loss were calculated by ray theory, assuming specular reflection with no loss from a single interface at the ocean bottom. The method is described by the expression [2]

BL = (H – Hcd + m)/n

Where *BL* is the bottom loss (in dB), *H* and *Hcd* are the measured bottom bounce propagation loss and calculated water column loss along the path; n is the order of the bottom loss bounce paths (*n*=1 in our case). The first bounce bottom only was used. The *m*(dB) correction is supposed to account for the number of first bottom interacting paths. These paths are associated with each order of bottom bounce. A random phase contribution from signals was assumed. No correction was made in this work as only the first arrival was taken into consideration.

The waveform used for the direct path arrivals was estimated from close range measurements of the acoustic source. This waveform was scaled using a sinx/x interpolation to compensate for the effects of small variations in explosion depth observed between the generated direct path signal and the received signal from each shot deployed in the propagation run.

Transfer Function

First of all we present bottom reflectivity in terms of a bottom transfer function, for number of traces from each shot (Figure 4a and 4b).
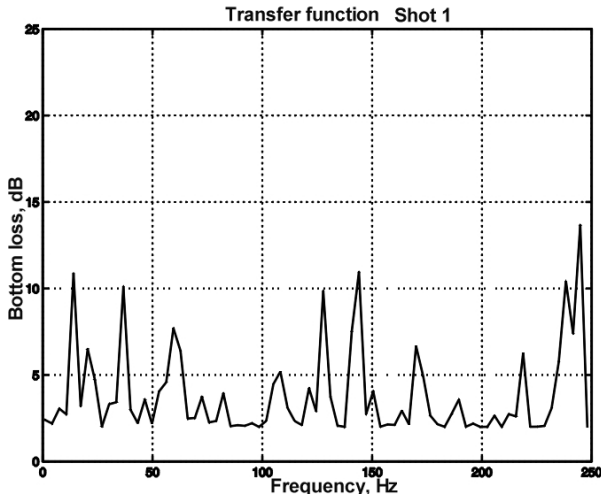
Transfer function   Shot 1

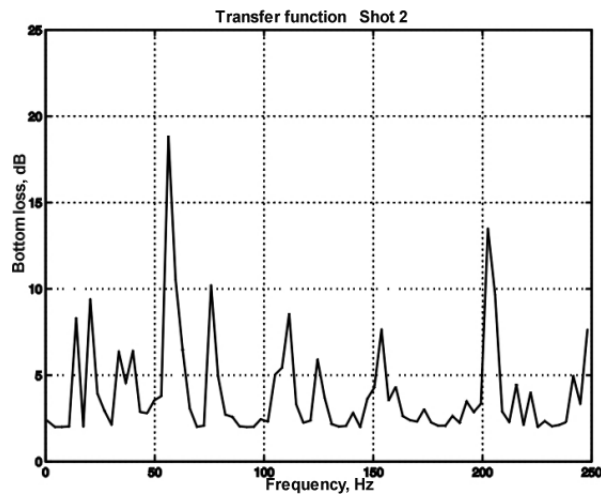Figure 4a. Transfer function. Shot 1.

Transfer function   Shot 2

Figure4b. Transfer function. Shot 2.

The transfer function is formed from the ratio of the Fourier transform of the reflected signal to the Fourier transform of the incident signal [4]. By means of this formulation, the bottom loss can be expressed in the frequency domain as is shown in Figures 5a-5b for a 30^0 grazing angle. The rapid variations in bottom loss are characteristic of an interference phenomenon produced by reflections off multiple sub-bottom layers. The loss curve was obtained by reading the peak level output from the multiple filter.

Bottom loss

Bottom loss variations are presented as a function of grazing angle for different frequencies that cover the frequency range from 40 to 240Hz. The calculated reflection (bottom loss: *-20 log |R|*) exhibits in general a complicated structure consisting of more or less regular sequence of peaks and dips.

The bottom reflection loss were calculated at frequencies 40, 80, 100, 140, 180 and 220Hz respectively for three different shots. Figure 5a, 5b and 5c show the bottom reflection loss versus grazing angle at frequencies 40, 80, and 220Hz respectively. Picks at these frequencies can be attributed to resonance phenomena of some sort. The distributions and widths of the resonance peaks contain the information about the interacting medium involved.
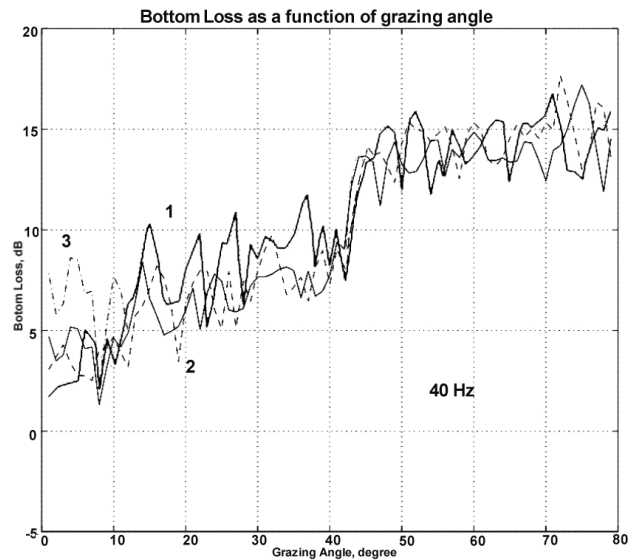
Bottom Loss as a function of grazing angle

Figure 5a. Bottom loss a function of grasing angle calculated at 40 Hz
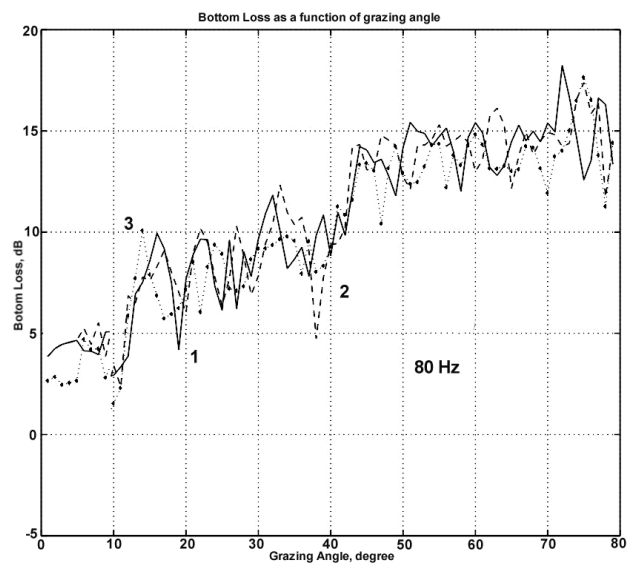
Bottom Loss as a function of grazing angle

Figure 5b. Bottom loss as function of grazing angle, calculated at 80 Hz

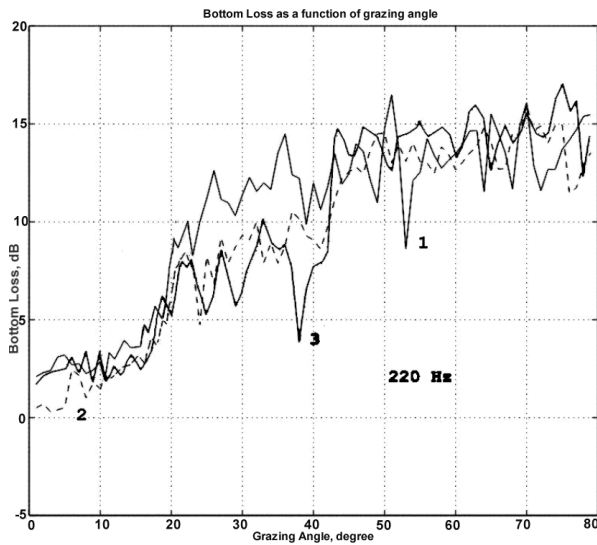Figure 5c. Bottom loss as afunction of grazing angle calculated at 220 Hz

Figure 6. Three dimensional representation of bottom loss calculations as function of grazing angle and frequency for Shot 1.

In the bottom loss results, a critical angle is observed which decreases from about 39^0 at 40-10 Hz to about 20^0 at 220 Hz. This critical angle is probably associated with the reflection of compressional waves near the ocean-sediment interface. The frequency dependence indicates that the lower frequencies interact with a deeper sediment layer of greater sound speed than the near-surface sediments. At about 59^0 there is a small indication of another critical angle, possibly due to reflection from the substrate beneath the sediments.

Based on these observations, it appears that the bottom loss contains relevant information about the structure and properties of the interacting medium.

The cause of the unpredictable variations of bottom loss is probably fine-scale sub-bottom layering. Averaging of the bottom loss results along segments of the seismic trackline will probably smooth the variations.

Figure 6, 7 and 8 present a three dimensional surfaces that summarie *Bottom Loss* as a function of both grazing angle and frequencies for one shot.
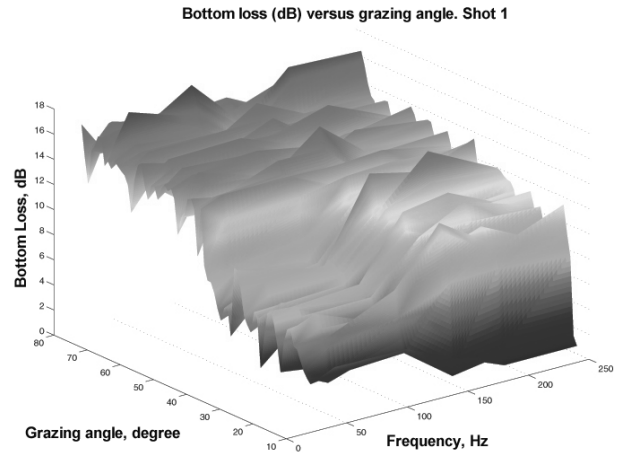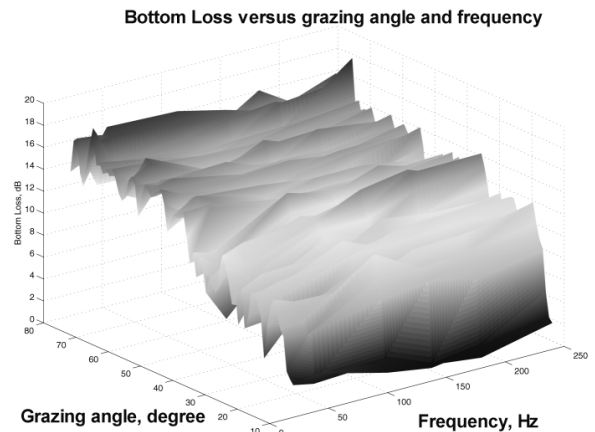

Figure 7. Three dimensional representation of bottom loss calculations as function of grazing angle and frequency for Shot 2.
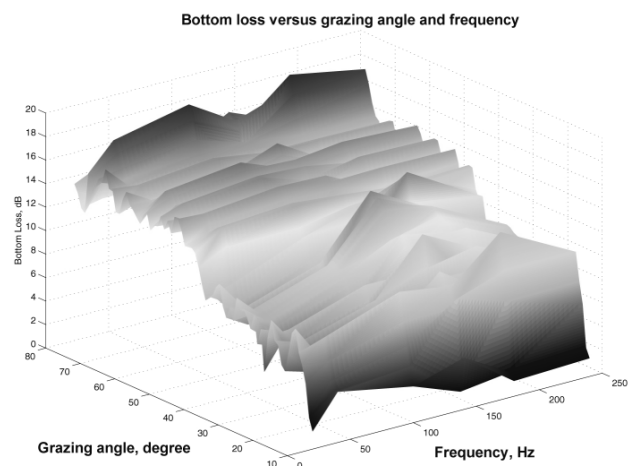

Figure 8. Three dimensional representation of bottom loss calculations as function of grazing angle and frequency for Shot 3.

Future steps

The next stage in development is to use the bottom loss structure to calculate some of the geoacoustic properties (velocities, porosities, attenuations) of the sediments, i.e. to solve the inverse reflection problem. Several smaller issues remain for additional work: the effect of the sea surface on far field source signature and the possibility of obtaining results for the very low grazing angles ($<10^0$) despite refraction effects.

Acknowledgements

References

1. AGSO, 1997. Reflection seismic data. Unpublished Technical Report.

2. Chapman, N.R., 1980. Low frequency bottom reflectivity measurements in the Tufts Abyssal Plain. In: Kuperman, W.A. & Jensen, B. (Eds) Bottom-interacting ocean Acoustics, New-York.

3. Dziewonsky, A., Bloch, S. and Lindsman, M., 1969. 'A Technique for the Analysis of Transient Seismic Signals'. Bull. Seism. Soc. Am., 59(1), p. 427-444.

4. Hanrahan, J.J. 1980. A perspective on bottom reflectivity and backscattering. In: Kuperman, W.A. & Jensen, B. (Eds) Bottom-interacting ocean Acoustics, New-York.

5. Spofford, C.W. Inference of Geo-Acoustic parameters from bottom-loss data. In: Kuperman, W.A. & Jensen, B. (Eds) Bottom-interacting ocean Acoustics, New-York.

6. Kritski, A. 1999. Extraction of Acoustical Properties of Sediments from Reflection Seismic Data: 1. Proposed Methods. Sydney University Ocean Sciences Institute Report, 85, 1-4.

7. Kritski, A. & Jenkins, C.J. 1999. Extraction of acoustical properties of sediments from reflection seismic data: 2. Data reading & display. Sydney University Ocean Sciences Institute Report, 86, 1-16.

8. Stoll, R.D. & Kan, T.K., 1981. Reflection of acoustic waves at the water-sediment interface. J.Acoust. Soc.Am., 70(1), 149-155.